



## Operations on Signed Distance Function Estimates

Csaba Bálint<sup>1</sup> , Gábor Valasek<sup>2</sup> , Lajos Gergő<sup>3</sup> 

<sup>1</sup>Eötvös Loránd University, [csabix@inf.elte.hu](mailto:csabix@inf.elte.hu)

<sup>2</sup>Eötvös Loránd University, [valasek@inf.elte.hu](mailto:valasek@inf.elte.hu)

<sup>3</sup>Eötvös Loránd University, [gergo@inf.elte.hu](mailto:gergo@inf.elte.hu)

Corresponding author: Csaba Bálint, [csabix@inf.elte.hu](mailto:csabix@inf.elte.hu)

**Abstract.** Signed distance functions (SDF) are versatile shape representations and challenging to realize as Lipschitz division and minimum/maximum CSG operations do not generally yield an exact distance representation. On the other hand, signed distance lower bounds are convenient for modeling as they are closed under the above operations, yet the sphere tracing algorithm may not converge for the resulting distance estimate.

In this paper, we first show that, under certain conditions, the CSG operations are closed under sphere tracing convergence; that is, if the algorithm converges on the primitives, it will converge on any CSG tree assembled from them. Second, we quantify the precision loss for each operation and region of space through the notion of set-contact smoothness, a generalized angle of intersection of surfaces.

**Keywords:** Computer graphics, Signed distance function, Distance estimate, Sphere Tracing  
**DOI:** <https://doi.org/10.14733/cadaps.2023.1154-1174>

## 1 INTRODUCTION

Our paper presents a general theoretical framework to investigate the quantitative aspects of bounding distance functions. In practice, distance function representations are rarely exact, yet most mathematical foundations are either generalized for any implicit function or only applicable to exact distance representations. Our research aims to close this gap.

We propose a precision definition for quantifying the accuracy of the min/max representation of set-theoretic operations in the entire space and show how the precision and the geometric configuration of the arguments determine the accuracy of the resulting approximation. The Lipschitz division is a practical technique for distance estimation, but it often yields imprecise results. This paper analyzes such estimates and states how set-operations can further degrade the precision of the distance representation.

For example, the minimum of two exact signed distance functions (SDF) that describes the union of two objects is often treated as another exact signed distance function. However, the resulting function is not an

exact SDF, and the error can be arbitrary large under certain conditions, as visualized in Figure 1. Similarly, representing the result of an intersection via the maximum operation or the offset geometry by subtraction is no longer an exact SDF; the former is demonstrated in Figure 2.

In addition, the theorems presented here can be applied in an arbitrary geometrical context. The propositions only impose conditions on the implicit mappings used to represent the particular set of points. As such, they hold for objects with or without volumes, implicit curves in space, non-differentiable or non-manifold surfaces, fractals, and any combination of these. Despite the generality, our theorems show that the sphere tracing algorithm retains convergence under set-theoretic union and intersection operations, a result for which such a general derivation has not yet been presented.

We prove our results on a subset of Hart's signed distance lower bounds called signed distance function estimates (SDFE). Despite this, most so-called *distance estimates* used by the industry and the online creative coding communities such as ShaderToy are SDFEs, placing no practical restrictions on the applicability of our results. This means that any Constructive Solid Geometry (CSG) tree made from SDF primitives and such set-operations will, in general, retain sphere tracing convergence in CAD systems such as nTopology [1]. Our theoretical framework allows the analysis of general argument geometries via a function that quantifies intersection smoothness at various scales.

## 1.1 PREVIOUS WORK

This paper mostly builds upon three previous theoretical results. Firstly, Hart [17] devised the sphere tracing algorithm for signed distance lower bounds. Hart also formulated a mathematical framework for modeling surfaces by defining set-operations and various primitives to build CSG trees [11]. He Provided a strong theoretical foundation with an efficient rendering algorithm and inspired numerous rendering techniques and modeling methods [29, 12, 19, 4, 15, 3], and their applications in computer-aided geometric design and modeling, computer graphics, and physics [16, 28, 10, 2, 23, 14].

Secondly, this paper is an extension to the papers by Bálint and Valasek et al. [12, 27]. They investigated the SDF offset operation, which mostly retains the exact distance representation in [12], and they attempted to define exact set-operations by replacing the SDF representation to footpoint mapping or boundary projection [27]. Unfortunately, the former paper lacks any description of the resulting function properties inside the offset, while the latter lacks the mathematical background to support the need for the algorithm.

Signed distance functions are powerful implicit representations, adapted for a wide range of applications such as computer-aided geometric design and modeling, computer graphics, and physics [16, 28, 10, 2, 23, 14].

Even though these functions offer attractive theoretical and practical properties, constructing exact distance functions to free-form surfaces is intractable in closed form [21, 5, 6, 27]. As a result, one must use approximate distance functions, for which a variety of approaches have been presented in the literature. These include sampling and filtering [13], piece-wise approximations [26], machine learning [24, 20], and devising bounds to the actual distance mapping [17]. Our paper focuses on the latter, that is, on the investigation of distance bound functions that are defined on the entire space.

Hart showed that the properties of signed distance lower bounds lead to a robust and efficient direct visualization method in [17]. He also proved that signed distance lower bounds are closed under minimum and maximum operations, which are the implicit representations of the result of intersection and union of implicit geometries [25]. Figures 1 and 2 visualize how the distance estimate becomes inaccurate under these operations.

Moreover, Ricci noted that one could construct signed distance lower bounds by dividing a Lipschitz continuous implicit function by any of its Lipschitz constants. However, contrary to the common intuition, the Lipschitz constants cannot be used to quantify the precision of the distance estimation: Lipschitz continuity does not imply the convergence of the sphere tracing algorithm.

Biswas and Shapiro proposed the use of the order of normalization to quantify the accuracy of distance

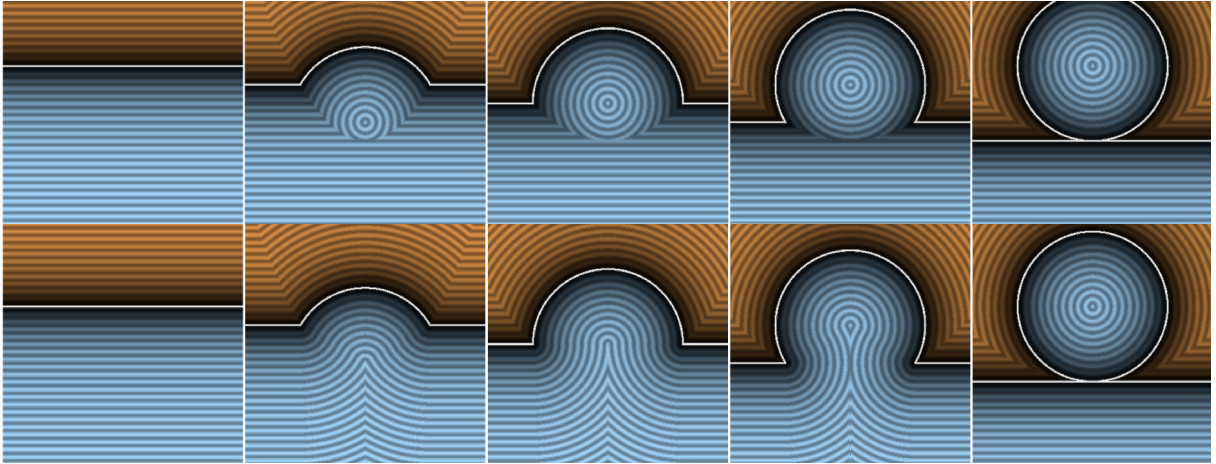


**Figure 1:** Comparison of distance estimate (top row) and exact signed distance values (bottom row) of a union of a circle and a half-plane in 2D with various distances between. The estimate is exact on the outside regions (orange), but inaccurate inside the union (blue) in the middle three images. The distance estimate of the union is the minimum of the exact signed distances to the circle and half-plane.

approximation close to the boundaries. They presented a detailed analysis of the quality of approximation in [8], relying on an initial polygonization of the input geometry.

**Outline** The following section contains a brief notational and theoretical summary of the most relevant mathematical results for this paper.

Section 3 reviews the practical anchor for our investigation, Hart’s sphere tracing algorithm. The precision of distance approximation directly affects the computational cost of ray-surface intersections, giving us an intuitive geometric setting in which we can interpret our theoretical results. We also present a signed and unsigned distance function definition.

A wider family of functions is introduced and investigated in Section 5 called signed distance function estimates (SDFE). Such a distance estimate has convergence guarantees for sphere tracing, yet they can be constructed efficiently for most surfaces. Our main contribution, a unified investigation of how bounds behave when intersecting SDFEs, is presented throughout Sections 6, 7, and 8. The intersection theorem is divided into four theorems that describe the behavior of the SDFE on different subsets of space.

Section 9 summarizes and generalizes the four theorems into one unifying set-operation theorem, including union, intersection, and set-difference.

## 2 PRELIMINARIES

Let  $(\mathbb{R}^3, d)$  denote a Euclidean metric space with  $d : \mathbb{R}^3 \times \mathbb{R}^3 \rightarrow [0, +\infty]$ . We utilize the same symbol for point-to-set and set-to-set distance:  $d(\mathbf{p}, \emptyset) = +\infty$ ,  $d(\mathbf{p}, A) := \inf_{\mathbf{a} \in A} d(\mathbf{p}, \mathbf{a})$ , and  $d(A, B) := \inf_{\mathbf{a} \in A} d(\mathbf{a}, B)$  for all  $\mathbf{p} \in \mathbb{R}^3, \emptyset \neq A, B \subseteq \mathbb{R}^3$ . Note that set-to-set distance is not a metric, but it is symmetric and positive.

We denote the  $r > 0$  neighborhood of a  $\mathbf{p} \in \mathbb{R}^3$  point by the  $\mathcal{K}_r(\mathbf{p}) := \{\mathbf{x} \in \mathbb{R}^3 \mid d(\mathbf{x}, \mathbf{p}) < r\}$  open set.  $A \subseteq \mathbb{R}^3$  set is open if  $\forall \mathbf{a} \in A, \exists \epsilon > 0 : \mathcal{K}_\epsilon(\mathbf{a}) \subseteq A$ .  $B \subseteq \mathbb{R}^3$  is closed if its complementary set,  $\mathbb{R}^3 \setminus B$ , is open. A set is bounded if there exists  $\mathcal{K}_r(\mathbf{p})$  that covers it. The diameter of a bounded  $\emptyset \neq C \subseteq \mathbb{R}^3$  set is a real number defined as  $\text{diam } C := \sup\{d(\mathbf{x}, \mathbf{y}) \mid \mathbf{x}, \mathbf{y} \in C\}$ .

**Lemma 1** (Existence of extrema). *If  $A \subseteq \mathbb{R}^3$  is closed and  $\mathbf{p} \in \mathbb{R}^3$ , then  $\exists \mathbf{a} \in A : d(\mathbf{p}, A) = d(\mathbf{p}, \mathbf{a})$ . [18]*

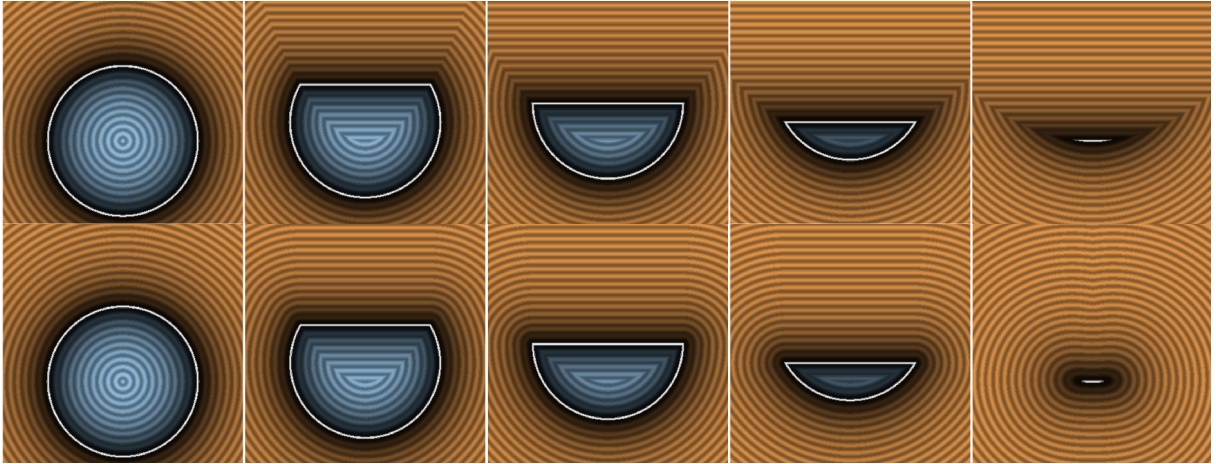


**Figure 2:** Comparison of distance estimate (top row) and exact signed distance values (bottom row) of the intersection of a circle and a half-plane in 2D with various distances between. The estimate is exact on the inside regions (blue), but inaccurate outside the intersection (orange) in all but the leftmost image. The distance estimate of the intersection is the maximum of the exact signed distances to the circle and half-plane.

Furthermore, we denote the interior of the set  $A \subseteq X$  as  $\text{int } A := \{\mathbf{a} \in A \mid \exists \epsilon > 0 : \mathcal{K}_\epsilon(\mathbf{a}) \subseteq A\}$ . The closure of the set  $A \subseteq X$  is denoted as  $\bar{A} := \{\mathbf{a} \in X \mid \forall \epsilon > 0 : \mathcal{K}_\epsilon(\mathbf{a}) \cap A \neq \emptyset\}$ . The boundary set of  $A$  is denoted by  $\partial A := \bar{A} \setminus \text{int } A$ . For any set  $A \subseteq X$ , it is clear from the definitions that  $\text{int } A$  is open,  $\bar{A}$  and  $\partial A$  are closed sets.

**Definition 1** (Offset). For any  $D \subseteq \mathbb{R}^3$  the radius  $r \geq 0$  closed offset set from  $D$  is defined as  $\bar{\mathcal{K}}_r(D) := \{\mathbf{x} \in \mathbb{R}^3 \mid d(\mathbf{x}, D) \leq r\}$ .

The interior of  $\bar{\mathcal{K}}_r(D)$  is denoted as  $\mathcal{K}_r(D) := \text{int } \bar{\mathcal{K}}_r(D)$ . This equals to  $\{\mathbf{x} \in \mathbb{R}^3 \mid d(\mathbf{x}, D) < r\}$  if  $r > 0$ . The difference compared to the neighbourhood definition is to allow  $r = 0$  which opens the set. Offsetting is additive  $\mathcal{K}_{r_1}(\mathcal{K}_{r_2}(D)) = \mathcal{K}_{r_1+r_2}(D)$  ( $r_1, r_2 > 0$ ) due to the following theorem from [6]:

**Theorem 1** (Offset-theorem). If  $D \subseteq \mathbb{R}^3$  is closed and  $r \geq 0$ , then

$$d(\mathbf{p}, D) - r = d(\mathbf{p}, \mathcal{K}_r(D)) \quad (\forall \mathbf{p} \in \mathbb{R}^3 \setminus \mathcal{K}_r(D)).$$

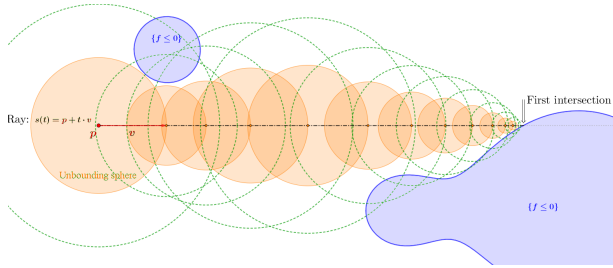
**Remark.** Our definition differs from the offset surface defined with translations along the normal because we may not have a normal or a surface. Therefore, the offset is the neighbourhood, and the offset surface is the boundary of that neighbourhood.

### 3 SPHERE TRACING

From now on, let us consider surfaces defined by an  $f : \mathbb{R}^3 \rightarrow \mathbb{R}$  implicit function, such that the surface is the  $\{f = 0\} := \{\mathbf{x} \in \mathbb{R}^3 \mid f(\mathbf{x}) = 0\}$  level-set. When denoting a function as  $f : A \rightarrow B$ , we assume that it is defined for all  $a \in A$ . A ray is a half line originating from a particular point  $\mathbf{p} \in \mathbb{R}^3$ , for example, the camera, towards a given unit length direction  $\mathbf{v} \in \mathbb{R}^3$ ,  $\|\mathbf{v}\|_2 = 1$ , denoted as:

$$\mathbf{s}(t) := \mathbf{s}_{\mathbf{p}, \mathbf{v}}(t) := \mathbf{p} + t \cdot \mathbf{v} \in \mathbb{R}^3 \quad (t \geq 0).$$

Therefore, the ray-surface intersection problem is expressed as finding the smallest positive root of the composite function  $f \circ \mathbf{s} : [0, +\infty) \rightarrow \mathbb{R}$ . Usually, we infer that  $f$  is continuous, or it at least has the



(a) Sphere tracing takes distance sized steps so it does not overstep a solution and converges quickly. The unbounding spheres (orange circles) contain no surface points while each of the green circles do, so  $f$  is an SDFE.

```

In :  $\mathbf{p}, \mathbf{v} \in \mathbb{R}^3, \|\mathbf{v}\|_2 = 1$  ray
        $f : \mathbb{R}^3 \rightarrow \mathbb{R}$  distance function
Out:  $t \in [0, +\infty)$ 
       distance traveled along the ray
 $t := 0; \quad i := 0;$ 
for  $i < i_{max}$  and
 $f(\mathbf{p} + t \cdot \mathbf{v})$  not too small do
  |  $t := t + f(\mathbf{p} + t \cdot \mathbf{v})$ 
  |  $i := i + 1$ 
end
return  $t$ 

```

(b) Sphere tracing adapted from [17].

**Figure 3:** Sphere tracing visualized in 2D (a) is a practical algorithm (b) for implicit surface rendering.

**Definition 2** (Bolzano-property). The function  $f : \mathbb{R}^3 \rightarrow \mathbb{R}$  is Bolzano if

$$\forall \mathbf{x}, \mathbf{y} \in \mathbb{R}^3 : f(\mathbf{x}) \cdot f(\mathbf{y}) \leq 0 \implies \exists \mathbf{z} \in \overline{\mathbf{x}\mathbf{y}} : f(\mathbf{z}) = 0.$$

where  $\overline{\mathbf{x}\mathbf{y}} = \{(1-t) \cdot \mathbf{x} + t \cdot \mathbf{y} \mid t \in [0, 1]\}$  is the segment connecting  $\mathbf{x}$  and  $\mathbf{y}$ .

Let us now consider the Banach-space  $(\mathbb{R}^3, \|\cdot\|_2)$  with the induced metric  $d(\mathbf{x}, \mathbf{y}) := \|\mathbf{y} - \mathbf{x}\|_2$  ( $\mathbf{x}, \mathbf{y} \in \mathbb{R}^3$ ).

**Definition 3** (Distance operator). Let us define the set to distance function operator  $\mathbf{D} : \mathcal{P}(\mathbb{R}^3) \setminus \{\emptyset\} \rightarrow C(\mathbb{R}^3, [0, +\infty))$  as

$$\mathbf{D}_A(\mathbf{p}) := d(\mathbf{p}, A) \quad (\emptyset \neq A \subseteq \mathbb{R}^3, \mathbf{p} \in \mathbb{R}^3),$$

where  $C(\mathbb{R}^3, [0, +\infty))$  is the set of continuous functions from  $\mathbb{R}^3$  to  $[0, +\infty)$ , and  $\mathcal{P}(\mathbb{R}^3)$  is the power set.

**Remark.** This operator denotes the implicit distance function representation for any set of points in space, including curves and surfaces. Thus, at every sample point the function  $\mathbf{D}_A$  evaluates to the distance from the surface of  $A$ . This leads us to the following properties:

1. The distance operator is invariant under closure, i.e.  $\forall \emptyset \neq A \subseteq \mathbb{R}^3 \implies \mathbf{D}_A = \mathbf{D}_{\overline{A}}$ .
2. However, the reverse is not necessarily true, i.e.  $\mathbf{D}_A \neq \mathbf{D}_{\text{int } A}$ . For example, if  $A$  is finite, then  $\text{int } A = \emptyset$ .
3.  $\mathbf{D}$  is bijective on the set of open sets. That is, if  $\emptyset \neq A, B \subseteq \mathbb{R}^3$  are open, then  $A = B \iff \mathbf{D}_A = \mathbf{D}_B$ .
4.  $\mathbf{D}$  is bijective on the set of closed sets. That is, if  $\emptyset \neq A, B \subseteq \mathbb{R}^3$  are closed, then  $A = B \iff \mathbf{D}_A = \mathbf{D}_B$ .

Luo et al. investigated the signed distance operator in more detail in their recent paper [21].

**Definition 4.**  $f : \mathbb{R}^3 \rightarrow \mathbb{R}$  is a *distance function* if  $f = \mathbf{D}_{\{f=0\}}$ .

**Example.** The open unit sphere has the following distance function:  $f_{\circ}(\mathbf{p}) = d(\mathbf{p}, \mathcal{K}_1(\mathbf{0})) = \max(\|\mathbf{p}\|_2 - 1, 0)$  ( $\mathbf{p} \in \mathbb{R}^3$ ).

**Definition 5** (Unbounding sphere). An unbounding sphere to the surface  $A$  at a given point  $\mathbf{p}$  is an open neighbourhood  $\mathcal{K}_r(\mathbf{p})$  where  $0 \leq r \leq \mathbf{D}_A(\mathbf{p})$ .

There are no surface points closer to  $\mathbf{p}$  than  $\mathbf{D}_A(\mathbf{p})$ , so  $\mathcal{K}_{f(\mathbf{p})}(\mathbf{p}) \cap \{f = 0\} = \emptyset$ . This property demonstrates that the sphere tracing algorithm can be applied to find the first ray-surface intersection. The algorithm on Figure 3b iteratively takes distance-sized steps along the ray; thus no ray-surface intersection is skipped while large empty spaces are traversed quickly as illustrated by Figure 3a.

The sphere tracing algorithm is not optimal; however, faster algorithms only differ in a constant factor [19, 4, 7, 15]. In this paper, we focus on operations on the implicit representations of surfaces and their effect on convergence speed rather than the algorithms or surfaces themselves.

## 4 SIGNED DISTANCE FUNCTIONS

**Definition 6** (SDF). If  $f : \mathbb{R}^3 \rightarrow \mathbb{R}$  is continuous and  $|f|$  is a distance function, then  $f$  is a signed distance function.

Here, the distance values of the function are augmented with a sign. This means that, from the perspective of the representation,  $\{f < 0\} := \{\mathbf{x} \in \mathbb{R}^3 \mid f(\mathbf{x}) < 0\}$  is the "inside" and the  $\{f > 0\} = \{-f < 0\}$  is the "outside" of the described geometry while either of these sets can be empty. Throughout the rest of the paper, we mean inside and outside as such, and the argument object will mean the nonempty set  $\{f \leq 0\} = \{f < 0\} \cup \{f = 0\}$ . For example,  $\mathbb{R}^3 \ni \mathbf{p} \mapsto \|\mathbf{p}\|_2 - 1 \in [-1, +\infty)$  is a signed distance function of the closed unit sphere.

Continuity in the definition is required to ensure that the SDFs are Bolzano functions, i.e., the signs do not change without crossing the surface. However, this does not imply that the signs have to change at  $\{f = 0\}$ , so distance functions are SDFs without interior ( $\{f < 0\} = \emptyset$ ) by our definition. Moreover, the definition implies that  $\{f = 0\} \neq \emptyset$ . Mathematically, the exact distance representations are important, and there are extensive studies that investigate signed distance functions [6], boundary projections [27], or both [21]. Practically, however, exact SDFs are infeasible for anything but the most trivial scenes.

Since signed distance values define solid objects, boolean operations on these implicit functions become practical for union, intersection, and subtraction to combine them into complex shapes. Taking the minimum distance values yields the union, and taking the maximum distance produces the implicit function of the intersection object. However, the result is not an exact SDF, as demonstrated on Figure 1 and 2. The shading is adapted from Íñigo Quílez [22]. To quantify how inaccurate the distance estimation is we introduce the SDFE in Section 5 and derive prevision bounds through Section 6 to 8.

A common way of obtaining a distance estimate from an implicit function is to divide it by one of its Lipschitz constants. We can generalize this to functions that are not Lipschitz continuous by using a more general divisor. To identify the necessary properties of this quantity, let us first derive an alternative definition to Hart's signed distance lower bounds from [17].

**Definition 7** (Lipschitz constant). Let  $f : \mathbb{R}^3 \rightarrow \mathbb{R}$  be arbitrary. We define the set of Lipschitz constants as

$$\text{Lip } f := \{L > 0 \mid \forall \mathbf{x}, \mathbf{y} \in \mathbb{R}^3 : |f(\mathbf{x}) - f(\mathbf{y})| \leq L \cdot d(\mathbf{x}, \mathbf{y})\}. \quad (1)$$

The function  $f$  is Lipschitz continuous if  $\text{Lip } f \neq \emptyset$ .

This implies that the smallest Lipschitz constant of an  $f$  signed distance function is 1, i.e.,

$$\forall f : \mathbb{R}^3 \rightarrow \mathbb{R} \text{ SDF} \quad : \inf \text{Lip } f = \min \text{Lip } f = 1.$$

**Definition 8** (Closer factor). For any  $f : \mathbb{R}^3 \rightarrow \mathbb{R}$  function, we define the set of closer factors as

$$\mathcal{C}f := \left\{ Q > 0 \mid |f| \leq Q \cdot \mathbf{D}_{\{f=0\}} \right\} \subseteq (0, \infty)$$

The less symbol on functions above should hold for all inputs, that is  $\forall x \in \mathbb{R}^3 : |f(x)| \leq Q \cdot \mathbf{D}_{\{f=0\}}(x)$ .

**Remark.** Therefore,  $\mathcal{C}f$  is the set of all positive numbers that scale the true distance function such that it is still larger than  $|f|$  at every point.  $\mathcal{C}f$  can be derived from the Lipschitz constant Definition 7 by restricting  $\mathbf{y}$  in Equation 1 such that  $\mathbf{y} \in \{f = 0\}$ . Moreover, closer factors have the following properties for any  $f : \mathbb{R}^3 \rightarrow \mathbb{R}$  and  $b \in \mathbb{R}$ :

1.  $\mathcal{C}f = \emptyset$  or  $\mathcal{C}f$  is an unbounded interval.
2.  $\text{Lip } f \subseteq \mathcal{C}f$ .
3.  $\text{Lip } bf = |b| \cdot \text{Lip } f$  and  $\mathcal{C}bf = |b| \cdot \mathcal{C}f$ .
4.  $\text{Lip}(f + b) = \text{Lip } f$ ; however,  $\mathcal{C}(f + b) \neq \mathcal{C}f$ .
5.  $\bigcap_{b \in \mathbb{R}} \mathcal{C}(f + b) = \text{Lip } f$ .

Note that the Lipschitz continuity is a much stronger requirement than having a non-empty closer factor set, i.e.  $\mathcal{C}f \neq \emptyset$ . For example, if  $\text{Lip } f \neq \emptyset$ , then  $f$  is differentiable almost everywhere, yet there are non-continuous  $g : \mathbb{R}^3 \rightarrow \mathbb{R}$  functions where  $\mathcal{C}g \neq \emptyset$ , e.g.:

$$g(x, y, z) = \begin{cases} x & \text{if } x \neq 1 \\ \frac{1}{2} & \text{if } x = 1 \end{cases} \implies \mathcal{C}g = [1, +\infty)$$

Then signed distance lower bounds of Hart [17] that have a consistent sign are defined as

**Definition 9** (Signed Distance Lower Bound). The  $f : \mathbb{R}^3 \rightarrow \mathbb{R}$  function is a signed distance lower bound if  $1 \in \mathcal{C}f$  and  $\text{sgn} \circ f \in C(\{f \neq 0\})$ .

The definition by Hart [17] only used the  $1 \in \mathcal{C}f$  condition, which ensures that  $f$  is a lower bound to the actual distance. We also stipulate that  $\text{sgn} \circ f \in C(\{f \neq 0\})$ , so that the resulting function retains the Bolzano property from Definition 2. Otherwise, one could take a distance function and redefine it at a single point to be  $-1$  times its original value taking a single point from the outside inside. Hence, the  $\text{sgn} \circ f \in C(\{f \neq 0\})$  condition guarantees inside  $\{\text{sgn} \circ f = -1\}$  and outside  $\{\text{sgn} \circ f = 1\}$  makes sense in relation to the surface without restricting geometric properties.

As Hart noted in [17], we can generate a signed distance lower bound by dividing a function by its Lipschitz constant. However, the introduction of closer factors allows for more:

**Corollary 1.** If  $f : \mathbb{R}^3 \rightarrow \mathbb{R}$ ,  $\mathcal{C}f \neq \emptyset$  and  $\text{sgn} \circ f \in C(\{f \neq 0\})$ , then for all  $Q \in \mathcal{C}f$  the function  $f/Q$  is a signed distance lower bound.

**Remark.** Lipschitz constants are typically computed by finding the largest magnitude of the gradient function; however, Lipschitz-continuity on the entire  $\mathbb{R}^3$  is a very restricting requirement. In most cases, like algebraic surfaces,  $f$  is Lipschitz-continuous only on the compact subsets of  $\mathbb{R}^3$ . For example, authors of [5] obtain signed distance lower bounds in those cases by finding an unbounding sphere such that its radius coincides with  $|f|/\min \text{Lip } f$  when  $f$  is restricted to the unbounding sphere.

## 5 SIGNED DISTANCE FUNCTION ESTIMATE

This section introduces SDFEs, a set of signed distance bounds that possess convergence guarantees for algorithms such as sphere tracing by bounding their worst case slowdown. To quantify this, let us define

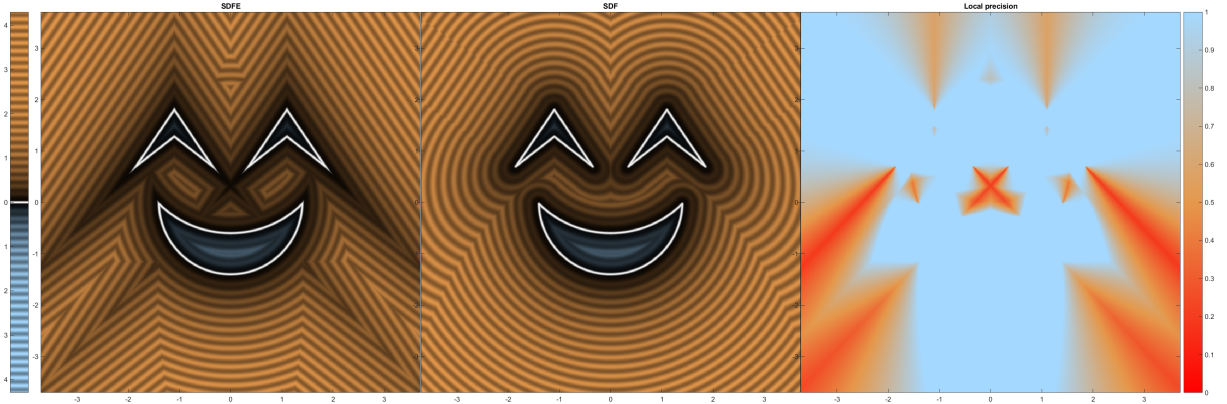


**Figure 4:** Left: SDFE obtained through min and max set operations using transformations of a half-plane (line) and a circle primitive. The ratio of the SDFE (left) and the exact SDF (middle) is displayed on the right. The right image shows that the precision of the final SDFE is around 0.2 at maximum. We prove that there is a lower bound to the precision and thus a maximum slowdown of the sphere tracing rendering algorithm.

**Definition 10** (Farther factors). For any  $f : \mathbb{R}^3 \rightarrow \mathbb{R}$ , let the set of farther factors be

$$\mathcal{F}f := \left\{ q > 0 \mid |f| \geq q \cdot \mathbf{D}_{\{f=0\}} \right\} \subseteq (0, +\infty).$$

**Remark.** Note that compared to closer factors, the relation sign is flipped meaning  $f$  is increasing at least  $q$  times more further away from the surface than the distance does. The  $\mathcal{F}f$  set is **unrelated to Lipschitz continuity** as it bounds the argument function from below with the actual distance. Let us summarize the properties of farther factors for a given  $f : \mathbb{R}^3 \rightarrow \mathbb{R}$ :

1.  $0 \notin \mathcal{F}f$ .
2.  $\mathcal{F}f$  is either empty or an interval with 0 as its left open end.
3.  $\mathcal{F}f \leq \mathcal{C}f$ , that is  $\forall q \in \mathcal{F}f, \forall Q \in \mathcal{C}f : q \leq Q$ .
4.  $\mathcal{F}f \cap \mathcal{C}f$  is empty or has a single element.
5.  $\mathcal{F}bf = |b| \cdot \mathcal{F}f$  for any  $b \in \mathbb{R}$ .

**Definition 11** (SDFE). The function  $f : \mathbb{R}^3 \rightarrow \mathbb{R}$  is a *signed distance function estimate* if  $\mathcal{F}f \neq \emptyset$ ,  $1 \in \mathcal{C}f$ , and  $\text{sgn} \circ f \in C(\{f \neq 0\})$

Note that SDFs are SDFEs as well, since  $\{1\} = \mathcal{F}f \cap \mathcal{C}f = (0, 1] \cap [1, \infty)$ . We call any  $q \in \mathcal{F}f$  a **precision of  $f$**  since  $0 < q \leq 1$  quantifies the difference between an exact SDF and our estimate, as demonstrated by Figure 4. Precision is also the maximum slowdown of the sphere tracing algorithm. This is the most distinct feature of SDFEs compared to signed distance lower bounds. More intuitive use of the farther factors is shown in the following Proposition. For the proof, the reader is referred to Appendix A.

**Proposition 1** (SDFE equivalence). For any  $f : \mathbb{R}^3 \rightarrow \mathbb{R}$  function and a fixed  $q \in (0, 1]$  number, the following statements are equivalent:

1.  $f$  is an SDFE with precision  $q \in \mathcal{F}f$

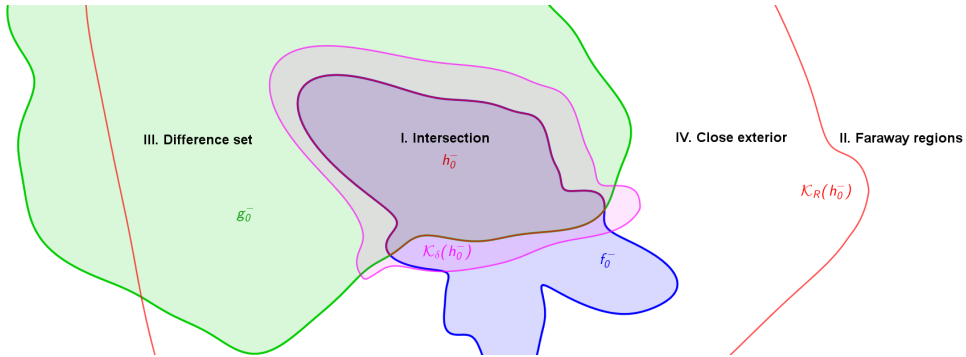


**Figure 5:** Partitions of space investigated by the proposed theorems. First, we prove the theorem on the intersection set, then on the far exterior. The third theorem sets bounds for the difference set, and finally, the fourth theorem applies to the close exterior.

2.  $\{f = 0\} \neq \emptyset$  and  $\text{sgn} \circ f$  is continuous on the  $\{f \neq 0\} \neq \emptyset$  set, and

$$\forall \mathbf{p} \in \mathbb{R}^3 : q \cdot d(\mathbf{p}, \{f = 0\}) \leq |f(\mathbf{p})| \leq d(\mathbf{p}, \{f = 0\}) \quad (2)$$

3.  $\exists \mu : \mathbb{R}^3 \rightarrow [1, \frac{1}{q}]$  bounded function such that  $f \cdot \mu$  is an SDF.

**Remark.** For any function and  $Q \in \mathcal{C} f$ , the open sphere centered at a  $\mathbf{p} \in \mathbb{R}^3$  point with radius  $\frac{f(\mathbf{p})}{Q}$  is an unbounding sphere. As such, it does not contain any surface points. However, for any  $q \in \mathcal{F} f$ , the  $\overline{\mathcal{K}}_{\frac{f(\mathbf{p})}{q}}(\mathbf{p})$  set is guaranteed to contain at least one surface point, as illustrated on Figure 3a with the green circles.

## 6 INTERSECTION-THEOREM: PART I

For all theorems that follow, let  $f$  and  $g$  denote signed distance function estimates (SDFEs) with precisions  $q_f \in \mathcal{F} f$  and  $q_g \in \mathcal{F} g$ , respectively. For simplicity, from this section on, the functions  $f : \mathbb{R}^3 \rightarrow \mathbb{R}$  may either mean the function or the set  $\{f = 0\} \subseteq \mathbb{R}^3$ . Let us also use the notational shorthands  $f_0^- := \{f \leq 0\}$  and  $f^- := \{f < 0\}$ . The  $f_0^+$  and  $f^+$  symbols are analogous. Minimum and maximum on functions are to be interpreted element-wise.

The most important theorem in the field comes from [17] that states how set-operations can be applied to objects defined by SDFs. Adapting our notation, Hart's theorem states that if  $f, g : \mathbb{R}^3 \rightarrow \mathbb{R}$  are such that  $1 \in \mathcal{C} f$  and  $1 \in \mathcal{C} g$ , then  $1 \in \mathcal{C} \min(f, g)$  and  $1 \in \mathcal{C} \max(f, g)$ , and therefore:

**Union:**  $\min(f, g)$  is a signed distance lower bound of the  $f_0^- \cup g_0^-$  object.

**Intersection:**  $\max(f, g)$  is a signed distance lower bound of  $f_0^- \cap g_0^-$ .

**Difference:**  $\max(f, -g)$  is a signed distance lower bound of  $f_0^- \setminus g_0^-$ .

Despite the practical robustness, Hart's set theorems do not show that the sphere tracing algorithm will still converge on the resulting estimate; for example, the lower distance bound set may be empty of the resulting function. Figure 4 demonstrates how precision drops as the result of the above set operations.

In the following four theorems, we provide a precision  $q \in \mathcal{F} \max(f, g)$  for the **intersection set operation**. The intersection theorem was subdivided into four theorems because the conditions and the techniques used change significantly depending on the subset of space that we investigate.

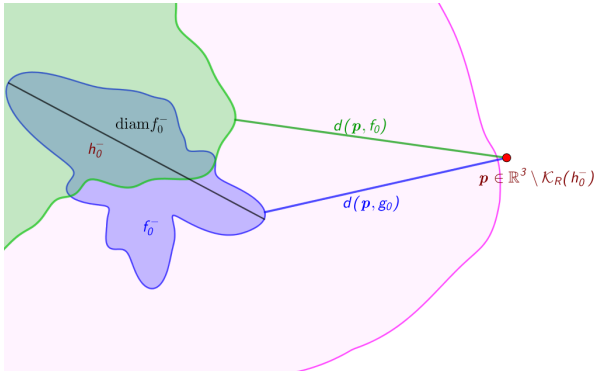


**Figure 6:** Intersection theorem when  $p$  is inside the intersection. The  $\max(f, g)$  function is the most precise within this region, as demonstrated by Figure 2.

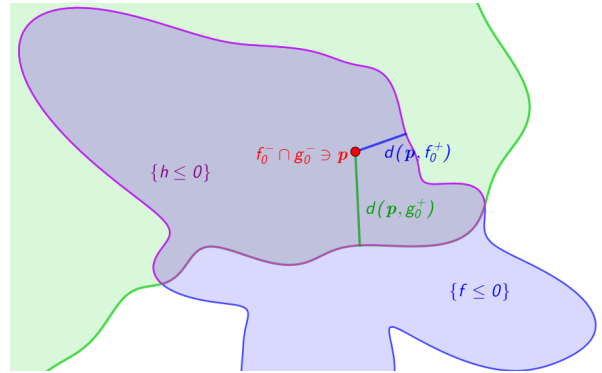


**Figure 7:** The theorem when  $p$  is far away from the intersection set. The estimation regains precision far from the surface in Theorem 3.

The intersection operation on SDFEs is expressed as the maximum of the two arguments denoted as

$$h := \max(f, g) := \mathbf{x} \mapsto \max(f(\mathbf{x}), g(\mathbf{x})) : \mathbb{R}^3 \rightarrow \mathbb{R} .$$

Since Hart has proved that  $h$  is a signed distance lower bound, we only have to show that  $\mathcal{F}h \neq \emptyset$ . For union and difference, the theorems can be reformulated using the de Morgan identities while considering the complement object defined by the SDFEs  $-f$  or  $-g$ . We summarize all of these corollaries in Section 10.

**Theorem 2** (Intersection theorem: Interior).  $h = \max(f, g)$  is an SDFE of the set  $h_0^- = f_0^- \cap g_0^-$  on the set  $h_0^-$  with the precision

$$\min(q_f, q_g) \in \mathcal{F}h \quad (q_f \in \mathcal{F}f, q_g \in \mathcal{F}g)$$

The proof is rather straightforward, see Appendix B for the details. Figure 6 provides a visual aid. The theorem states that within the intersection, the resulting SDFE  $h$  retains the precision of the less precise argument estimate.

Theorem 2 showed that intersection yields an SDFE that is as precise inside the intersection as the input distance estimates allow. However, the precision can be significantly lower on the exterior. The following sections investigate how precision drops as the two surfaces meet. Next, we prove that the bound tends toward that of the smaller object. Figure 7 depicts the situation when the neighborhood of the intersection is excluded from the SDFE bound calculation.

**Theorem 3** (Intersection-Theorem: Faraway). Suppose that  $f_0^-$  is bounded and  $R > \text{diam } f_0^-$ . Then  $h$  is an SDFE on  $\mathbb{R}^3 \setminus \mathcal{K}_R(h_0^-)$  with the precision

$$\frac{R - \text{diam } f_0^-}{R} q_f \in \mathcal{F}h \quad (q_f \in \mathcal{F}f) .$$

**Remark.** The proof is in Appendix C. Note that as  $R$  approaches infinity, the above tends to  $q_f$ . This means that at a distance, the SDFE of the bounded object determines the accuracy of the resulting SDFE.

If none of the surfaces  $\{f \leq 0\}$  and  $\{g \leq 0\}$  are finite, a counterexample on Figure 8 displays a scenario where the  $\mathcal{F}h = \emptyset$ . This 2D scene is the intersection of two unbounded objects  $f_0^-$  and  $g_0^-$ . Each object is a union of a half-plane and a circle. The intersections is the red bounded region and its distance function is poorly approximated with  $h = \max(f, g)$ , especially far away from  $h_0^-$ , causing sphere tracing to be slow.

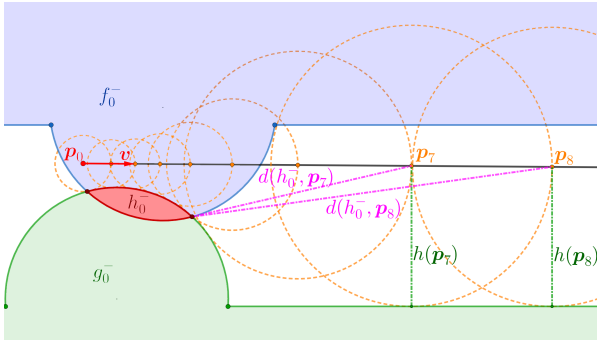


**Figure 8:** A counterexample for an intersection of two objects (blue & green) where both are unbounded and the maximum of their SDF is not an SDFE in Theorem 3. Here, sphere tracing does not accelerate for a diverging ray because  $\lim_{n \rightarrow \infty} h(p_n)/d(h_0, p_n) = 0$ .

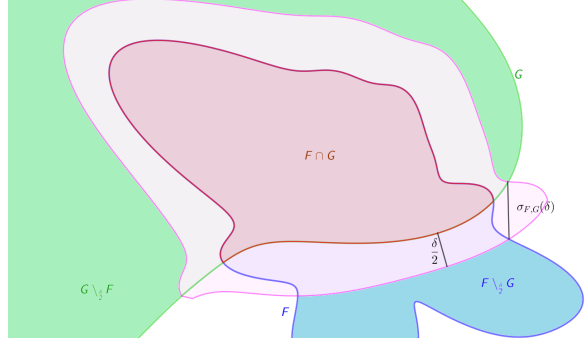


**Figure 9:** Set-contact smoothness  $\sigma_{F,G}(\delta)$  for a given  $\delta \geq 0$  is the distance between the offset difference sets  $F \setminus \mathcal{K}_{\frac{\delta}{2}}(F \cap G)$  and  $G \setminus \mathcal{K}_{\frac{\delta}{2}}(F \cap G)$ . This function describes the  $F \subseteq \mathbb{R}^3$  and  $G \subseteq \mathbb{R}^3$  sets geometric relation in various scales.

### 7 SET-CONTACT SMOOTHNESS

Our goal is to estimate the precision of the resulting  $h = \max(f, g)$  function close to the exterior of the surface  $\{h = 0\}$  without any geometric assumptions. However, the geometry of the intersection plays a vital role in the resulting precision. For this reason, we define a general set-contact smoothness modulus independent of both the geometric assumptions and the representation.

**Definition 12** (Offset difference of sets). The  $\delta \geq 0$  offset difference of sets  $F \subseteq \mathbb{R}^3$  and  $G \subseteq \mathbb{R}^3$  is

$$F \setminus_{\delta} G := F \setminus \mathcal{K}_{\delta}(F \cap G) .$$

The above shorthand notation for subtracting a little more from a set proved useful in the theorems that follow. The lemma below is an observation about the offset difference of objects, proved in Appendix D.

**Lemma 2.** Let  $F, G \subseteq \mathbb{R}^3$ ,  $\delta \geq 0$ , and  $p \in \mathbb{R}^3 \setminus \mathcal{K}_{\delta}(F \cap G)$ , then

$$\min \left( \frac{\delta}{2}, d(p, F \setminus_{\frac{\delta}{2}} G) \right) \leq d(p, F) . \tag{3}$$

**Definition 13.** Let  $F, G \subseteq \mathbb{R}^3$  be arbitrary sets. We define their contact smoothness modulus as the function

$$\sigma_{F,G}(\delta) := \min \left( \delta, d(F \setminus_{\frac{\delta}{2}} G, G \setminus_{\frac{\delta}{2}} F) \right) \quad (\delta \geq 0) .$$

For example, if  $F$  and  $G$  are two perpendicular intersecting lines,  $\sigma_{F,G}(\delta) = \frac{\sqrt{2}}{2}\delta$ . In general,  $\sigma_{F,G}$  quantifies how smoothly  $F$  and  $G$  melds on various scales.

**Proposition 2** (Properties). Let  $F, G \subseteq \mathbb{R}^3$ , then the following holds:

1.  $\sigma_{F,G}(0) = 0$
2.  $\sigma_{F,G}$  is a monotonically increasing function
3.  $\sigma_{F,G}(\delta) \leq \delta$

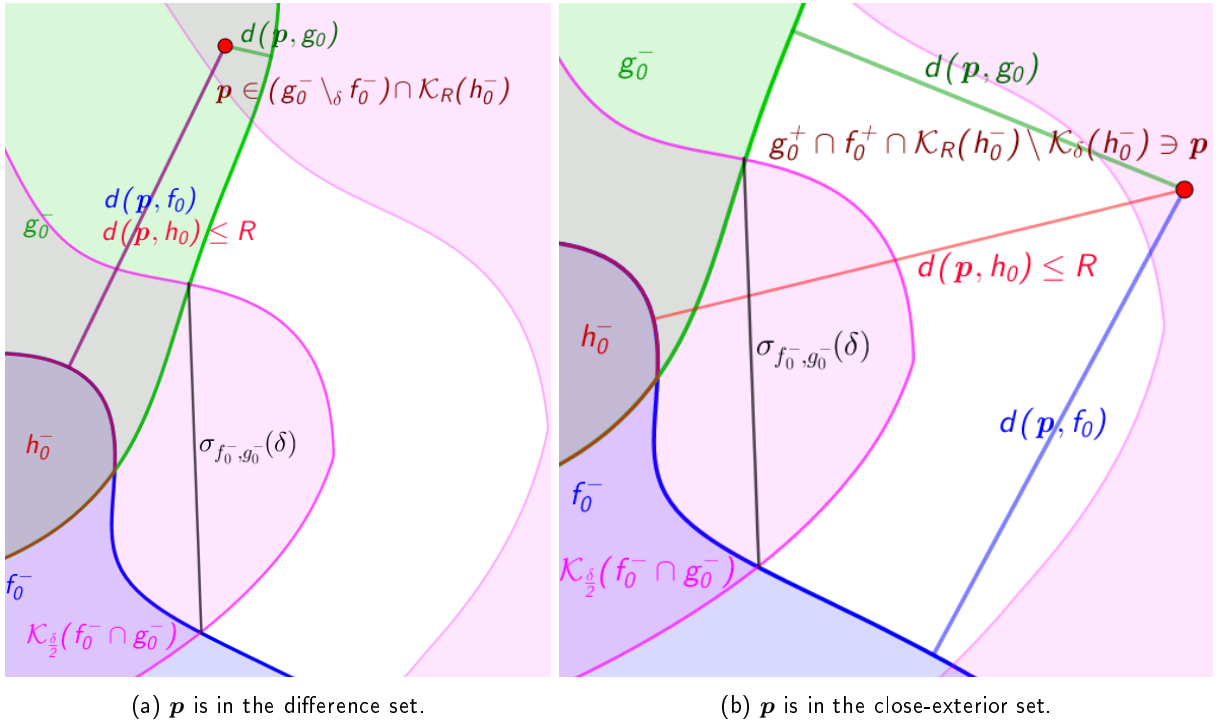


**Figure 10:** Visual aid for the proof of Theorem 4 and 5 located in Appendix F and G. In both cases, the set-contact smoothness of the argument geometries  $\sigma_{f_0^-, g_0^-}(\delta)$  aids the estimation of the precision.

4. If  $F$  and  $G$  are closed sets, then  $\forall \delta > 0 : \sigma_{F,G}(\delta) \neq 0$

*Proof.* Properties 1 and 3 follow from the definition. Property 2 holds since  $F \setminus_\delta G$  is also monotonic, so  $F \setminus_{\delta_1} G \subseteq F \setminus_{\delta_2} G$  if  $\delta_1 \leq \delta_2$ . The distance of sets is also monotonic, that is, the distance of subsets cannot decrease. Property 4 holds since if the remaining sets are non-empty, they remain closed and disjoint. The distance of closed and disjoint sets is non-zero.  $\square$

**Remark.** When one of the sets are not connected, the function  $\sigma_{F,G}^*(\delta) := d(F \setminus_{\frac{\delta}{2}} G, G \setminus_{\frac{\delta}{2}} F)$ , ( $\delta \geq 0$ ) can have a discontinuity and retain a higher value until  $\mathcal{K}_\delta(F \cap G)$  reaches the next component. Therefore, the  $\min(\delta, \cdot)$  is used in the equation allows the definition to make sense when  $\sigma_{F,G}^*$  is infinite, and it ensures that properties 1 through 3 hold. The following lemma allows us to estimate the precision in the two intersection theorems that follow. The proof is located in Appendix E.

**Lemma 3.** If  $F, G \subseteq \mathbb{R}^3$  are closed,  $\delta \geq 0$  and  $p \in \mathbb{R}^3 \setminus \mathcal{K}_\delta(F \cap G)$ , then

$$\frac{1}{2}\sigma_{F,G}(\delta) \leq \max(d(p, F), d(p, G))$$

## 8 INTERSECTION THEOREM: PART II

This section investigates how the intersection affects sphere tracing near the surface. We compute the precision of the SDFE in relation to the surface smoothness. First, we present our theorem on the difference set, which

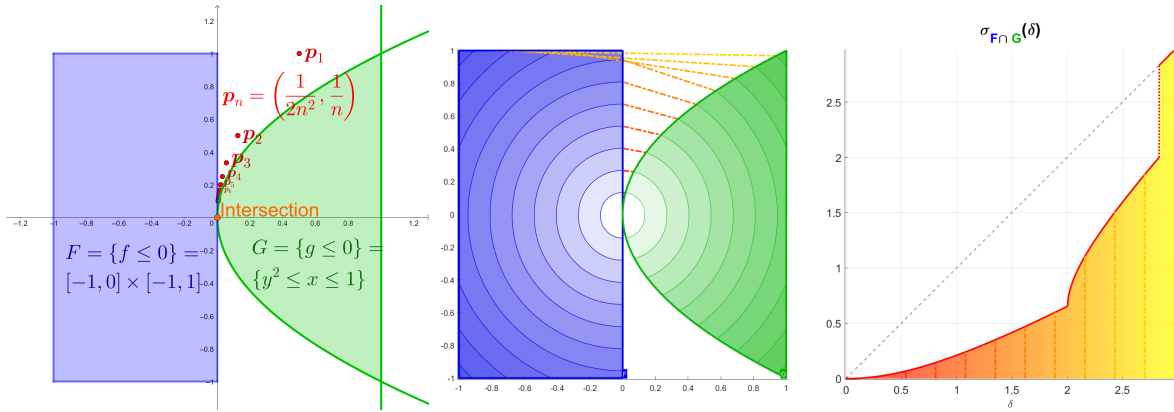


**Figure 11:** Counterexample (left, middle) for  $\delta = 0$  in Theorem 5. If the two surfaces join smoothly, then the sequence  $p_n = (\frac{1}{2n^2}, \frac{1}{n})$  converges faster to  $f_0^-$  and  $g_0^-$  than to  $h_0^- = \{(0, 0)\}$  resulting in  $\mathcal{F}h = \emptyset$ , so  $h = \max(f, g)$  is not an SDFE in this case. In practice, this decreases convergence rate because the set-contact smoothness function (right) has small values near the intersection. The middle image visualizes the distances (dashed lines) between the offset difference sets (shaded areas).

is followed by the theorem that provides a precision on the subspace of  $\mathbb{R}^3$  that is exterior to both argument objects.

Theorem 3 proved that the SDFE regains precision further away from the intersection. The following theorem focuses on the behavior of the SDFE close to the intersection surface within the difference set  $g_0^- \setminus_\delta f_0^-$  shown in Figure 10a.

**Theorem 4** (Intersection-theorem: Difference). *For every  $0 < \delta < R$  the function  $h = \max(f, g)$  is an SDFE on  $(g_0^- \setminus_\delta f_0^-) \cap \mathcal{K}_R(h_0^-)$ , with the precision:*

$$\frac{\sigma_{f_0^-, g_0^-}(\delta)}{R} \cdot q_f \in \mathcal{F}h \quad (q_f \in \mathcal{F}f) \tag{4}$$

The proof is in Appendix F. Assuming  $R \rightarrow \delta$ , the precision will be  $q_h \rightarrow \frac{\sigma(\delta)}{\delta} \cdot q_f$ , so 'smoother' surface connections, i.e. tangent surfaces, result in less precise SDFEs in the vicinity.

The final subset of space that we investigate is the near outside of the intersection, depicted in Figure 10b.

**Theorem 5** (Intersection-theorem: Exterior). *For every  $0 < \delta < R$  the function  $h := \max(f, g)$  is an SDFE on the exterior set  $((f_0^+ \cap g_0^+) \cap (\mathcal{K}_R(h_0^-) \setminus \mathcal{K}_\delta(h_0^-)))$  with the following precision:*

$$\frac{\sigma_{f_0^-, g_0^-}(\delta)}{2R} \cdot \min(q_f, q_g) \in \mathcal{F}h \quad (q_f \in \mathcal{F}f, q_g \in \mathcal{F}g) \tag{5}$$

The proof is located in Appendix G. In practice, the convergence speed of the sphere tracing algorithm depends on the  $\delta$  'near-threshold' distance, on the diameter of the smaller object  $\text{diam} f_0^-$ , and its SDFE bound  $K_f$ . The  $\delta$  appears in sphere tracing implementations as an arbitrarily small value used for a distance threshold under which the ray-surface intersection computation is terminated. This way, sphere tracing stops when the surface is sufficiently approximated, i.e. the error is smaller than a pixel.

**Remark.** If this near-threshold distance  $\delta$  is zero, the theorem does not hold as illustrated in Figure 11. The  $p_n := (\frac{1}{2n^2}, \frac{1}{n}) \in \mathbb{R}^2$ ,  $(n \in \mathbb{N})$  sequence is  $O(n^{-2})$  close to the two surfaces, but only  $O(n^{-1})$  close to their intersection set  $h_0^- = \{(0, 0)\}$  which means  $q_h > 0$  must be zero, thus  $\mathcal{F}h = \emptyset$ .

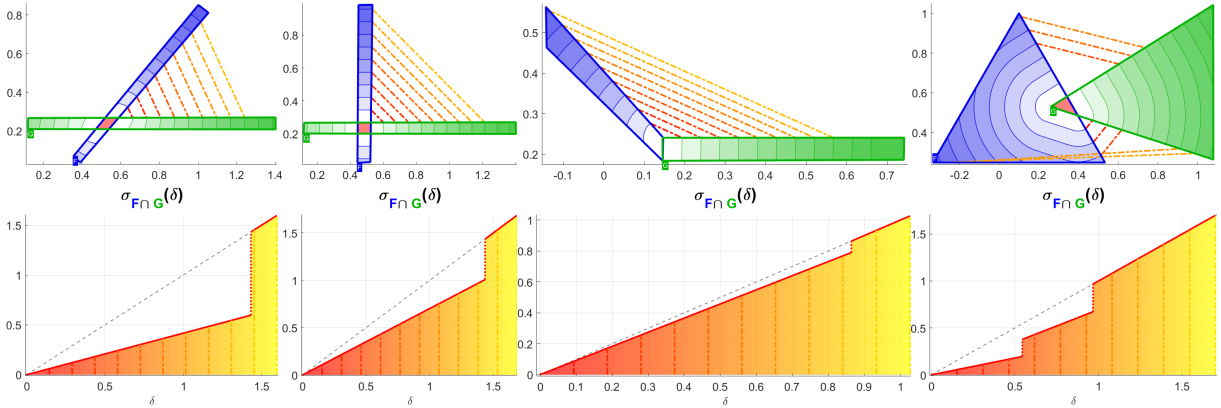


**Figure 12:** Examples for the set-contact smoothness modulus with different intersection angles in 2D. E.g., a 90° intersection results in  $\sigma_{F \cap G} = \frac{\sqrt{2}}{2} \delta$  as seen on the second and fourth images. Larger values in the modulus indicate a more accurate SDFE of the intersection.

### 9 RESULTS

We summarize our results in the following single theorem.

**Theorem 6 (Set operations).** *Suppose that  $f$  and  $g : \mathbb{R}^3 \rightarrow \mathbb{R}$  are SDFEs, and let  $0 < \delta \leq \text{diam}\{f = 0\}$ . Then, the following set-operations produce an SDFE with the function*

**Union**  $h = \min(f, g)$  for the  $f_0^- \cup g_0^-$  set if  $f_0^+$  is bounded

**Intersection**  $h = \max(f, g)$  for the  $f_0^- \cap g_0^-$  set if  $f_0^-$  is bounded

**Difference**  $h = \max(f, -g)$  for the  $f_0^- \setminus g_0^-$  set if  $f_0^-$  is bounded

with the precision

$$\frac{1}{4} \frac{\sigma_{\{f=0\}, \{g=0\}}(\delta)}{\text{diam}\{f = 0\}} \cdot \min(q_f, q_g) \in \mathcal{F}h \Big|_{\mathbb{R}^3 \setminus \mathcal{K}_\delta(\{h=0\})} \tag{6}$$

The theorem is proved in Appendix H. The theorem directly implies sphere tracing convergence on the resulting representation for the union, intersection, and difference operations. The theorem summarizes the previous ones and gives a single bound for a given near threshold distance. Unfortunately, this summarizing theorem is impractical for applications because the convergence rate depends on the size of the smaller set. Usually, the resulting SDFE is much more precise than this theorem guarantees because of the rough estimation that we used to get the global guarantee. For the above reasons, we must refer back to the individual intersection theorems since those can provide much better bounds individually.

However, the set-contact smoothness modulus only depends on the argument geometry and their relative position and indicates the precision loss quite well at various scales. The slope of this function indicates the angle at which the surfaces meet, as demonstrated by Figure 12. Our implementation can generate the set-contact smoothness modulus for 2D polygons but does so with a relatively brute-force approach. We adaptively sample the  $\sigma_{F \cap G}$  function using Chebfun [9] to find discontinuities and efficiently store the result. We found that small changes in shape or position can have a large effect on the modulus and the precision of the estimate, as seen in Figure 13.

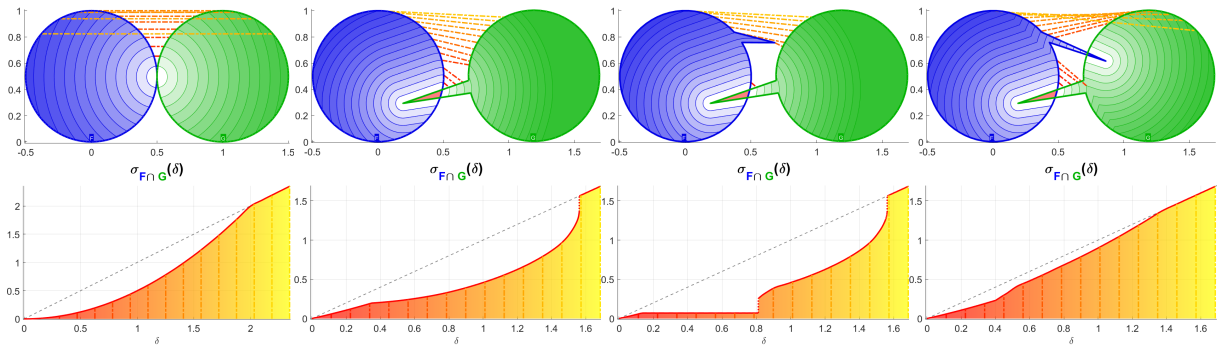


**Figure 13:** Additional examples for the set-contact smoothness modulus in 2D. Tangential (first) and almost intersecting surfaces (third) create the most inaccuracy in the signed distance function estimate.

## 10 CONCLUSION

This paper presented a subset of signed distance lower bound functions called signed distance function estimates (SDFE) with provable precision characteristics. These functions only pose constraints on the mapping and not on the represented geometry; as such, they can be applied in an arbitrary geometric context. In practice, the vast majority of signed distance approximations are also SDFEs.

We derived how the distance approximation accuracy can be obtained for the result of set-theoretic operations and how the SDFE representation of the argument geometries affects it via the closer and farther factors. We showed the quantitative effect of the relative geometric configuration of the arguments by introducing the set-contact smoothness modulus of arbitrary sets in space.

In particular, in Theorems 2, 3, 4, and 5, we have shown under which conditions are SDFEs closed under the intersection operation. Most importantly, the bound is determined by the contact of the argument surfaces in proximity to the resulting intersection surface. Another important factor is the diameter of the input geometries and the SDFE bound of the function that defines it implicitly.

In Section 9 we summarized our theoretical results for intersection, union, and set difference operations. We have concluded that apart from the contact smoothness of the argument geometries, the most deciding factor on the convergence speed of the sphere tracing algorithm is the subspace of  $\mathbb{R}^3$  in which the majority of the ray-tracing occurs.

In summary, we have proved that if these widely used distance bound set-operations are applied, the sphere tracing algorithms converges. This property was observed in practice but was not derived before.

Further research could investigate the optimization of a CSG tree since we formulated exact bounds for each operation. This CSG optimization would reorder operations and find better bounding volumes to minimize the resulting SDFE bound and computational cost, so the rays are computed most efficiently. Moreover, it would be interesting to analyze the various blending operations and their effect on SDFE precision.

## ACKNOWLEDGEMENTS

EFOP-3.6.3-VEKOP-16-2017-00001: Talent Management in Autonomous Vehicle Control Technologies – The Project is supported by the Hungarian Government and co-financed by the European Social Fund. Supported by the ÚNKP-21-3 New National Excellence Program of the Ministry for Innovation and Technology from the source of the National Research, Development and Innovation Fund.

## REFERENCES

- [1] Allen, G.: nTopology Modeling Technology, 2021. <https://ntopology.com/resources/whitepaper-implicit-modeling-technology/>.
- [2] Angles, B.; Tarini, M.; Wyvill, B.; Barthe, L.; Tagliasacchi, A.: Sketch-based implicit blending. *ACM Transactions on Graphics*, 36(6), 181:1–181:13, 2017. ISSN 0730-0301. <http://doi.org/10.1145/3130800.3130825>.
- [3] Bálint, C.; Kiglics, M.: A geometric method for accelerated sphere tracing of implicit surfaces. *Acta Cybernetica*, 2021. <http://doi.org/10.14232/actacyb.290007>.
- [4] Bálint, C.; Valasek, G.: Accelerating Sphere Tracing. In O. Diamanti; A. Vaxman, eds., *EG 2018 - Short Papers*. The Eurographics Association, 2018. ISSN 1017-4656. <http://doi.org/10.2312/egs.20181037>.
- [5] Bálint, C.; Valasek, G.: Interactive Rendering Framework for Distance Function Representation. *Annales Mathematicae et Informaticae*, 48, 5–13, 2018. ISSN 1787-6117. <http://ami.ektf.hu/index.php?vol=48>.
- [6] Bálint, C.; Valasek, G.; Gergó, L.: Operations on signed distance functions. *Acta Cybernetica*, 24(1), 17–28, 2019. <http://doi.org/10.14232/actacyb.24.1.2019.3>.
- [7] Bán, R.; Bálint, C.; Valasek, G.: Area Lights in Signed Distance Function Scenes. In P. Cignoni; E. Miguel, eds., *Eurographics 2019 - Short Papers*. The Eurographics Association, 2019. ISSN 1017-4656. <http://doi.org/10.2312/egs.20191021>.
- [8] Biswas, A.; Shapiro, V.: Approximate distance fields with non-vanishing gradients. *Graphical Models*, 66(3), 133–159, 2004. <http://doi.org/10.1016/j.gmod.2004.01.003>.
- [9] Driscoll, T., Hale: *Chebfun Guide*. Pafnuty Publications, Oxford, 2014.
- [10] Evans, A.: Learning from failure: a survey of promising, unconventional and mostly abandoned renderers for 'dreams ps4', a geometrically dense, painterly ugc game. In *Advances in Real-Time Rendering in Games*. MediaMolecule, SIGGRAPH, 2015.
- [11] Foley, J.D.: *12.7 Constructive Solid Geometry*, 533–558. Addison-Wesley Professional, 1990. ISBN 9780201848403.
- [12] Friedrich, M.; Roch, C.; Feld, S.; Hahn, C.; Fayolle, P.A.: A flexible pipeline for the optimization of CSG trees. *Computer Science Research Notes*, 2020. <http://doi.org/10.24132/csrn.2020.3001.10>.
- [13] Frisken, S.F.; Perry, R.N.; Rockwood, A.P.; Jones, T.R.: Adaptively sampled distance fields: A general representation of shape for computer graphics. In *Proceedings of the 27th Annual Conference on Computer Graphics and Interactive Techniques, SIGGRAPH '00*, 249–254. ACM Press/Addison-Wesley Publishing Co., New York, NY, USA, 2000. ISBN 1-58113-208-5. <http://doi.org/10.1145/344779.344899>.
- [14] Fuhrmann, A.; Sobotka, G.; Groß, C.: Distance fields for rapid collision detection in physically based modeling. *International Conference Graphicon 2003*, 2003.
- [15] Galin, E.; Guérin, E.; Paris, A.; Peytavie, A.: Segment tracing using local lipschitz bounds. *Computer Graphics Forum*, 39(2), 545–554, 2020. <http://doi.org/https://doi.org/10.1111/cgf.13951>.
- [16] Green, C.: Improved alpha-tested magnification for vector textures and special effects. In *ACM SIGGRAPH 2007 Courses, SIGGRAPH '07*, 9–18. ACM, New York, NY, USA, 2007. ISBN 978-1-4503-1823-5. <http://doi.org/10.1145/1281500.1281665>.
- [17] Hart, J.: Sphere tracing: A geometric method for the antialiased ray tracing of implicit surfaces. *The Visual Computer*, 12, 1995. <http://doi.org/10.1007/s003710050084>.
- [18] Hutchinson, J.E.: *Introduction to Mathematical Analysis*, 101–103. Australian National University Lecture Notes, 1994.

- [19] Keinert, B.; Schäfer, H.; Korndörfer, J.; Ganse, U.; Stamminger, M.: Enhanced Sphere Tracing. In A. Giachetti, ed., Smart Tools and Apps for Graphics - Eurographics Italian Chapter Conference. The Eurographics Association, 2014. ISBN 978-3-905674-72-9. <http://doi.org/10.2312/stag.20141233>.
- [20] Liu, S.; Zhang, Y.; Peng, S.; Shi, B.; Pollefeys, M.; Cui, Z.: DIST: rendering deep implicit signed distance function with differentiable sphere tracing. CoRR, abs/1911.13225, 2019. <http://arxiv.org/abs/1911.13225>.
- [21] Luo, H.; Wang, X.; Lukens, B.: Variational analysis on the signed distance functions. Journal of Optimization Theory and Applications, 180, 2019. <http://doi.org/10.1007/s10957-018-1414-2>.
- [22] nigo Quílez, I.: 2d distance functions. <https://iquilezles.org/articles/distfunctions2d/>.
- [23] Osher, S.; Fedkiw, R.: Signed distance functions. In Level Set Methods and Dynamic Implicit Surfaces, 17–22. Springer Verlag, 2003.
- [24] Park, J.J.; Florence, P.; Straub, J.; Newcombe, R.; Lovegrove, S.: Deepsdf: Learning continuous signed distance functions for shape representation. In The IEEE Conference on Computer Vision and Pattern Recognition (CVPR), 2019.
- [25] Ricci, A.: A Constructive Geometry for Computer Graphics. The Computer Journal, 16(2), 157–160, 1973. <http://doi.org/10.1093/comjnl/16.2.157>.
- [26] Song, X.; Jüttler, B.; Poteaux, A.: Hierarchical spline approximation of the signed distance function. In 2010 Shape Modeling International Conference, 241–245, 2010. <http://doi.org/10.1109/SMI.2010.18>.
- [27] Valasek, G.; Bálint, C.; Leitereg, A.: Footvector representation of curves and surfaces. Acta Cybernetica, 2021. <http://doi.org/10.14232/actacyb.290145>.
- [28] Wright, D.: Dynamic occlusion with signed distance fields. In Advances in Real-Time Rendering in Games. Epic Games (Unreal Engine), SIGGRAPH course, 2015.
- [29] Wyvill, B.; Guy, A.; Galin, E.: Extending the CSG Tree. Warping, Blending and Boolean Operations in an Implicit Surface Modeling System. Computer Graphics Forum, 1999. ISSN 1467-8659. <http://doi.org/10.1111/1467-8659.00365>.

# APPENDICES

## A PROOF OF SDFE EQUIVALENCE

*Proof of Proposition 1. 1.⇒2.* is trivial.

*2.⇒3.* Since  $\{f = 0\} \neq \emptyset$ , let  $\mu(\mathbf{p}) := 1$  ( $\mathbf{p} \in \{f = 0\}$ ),

$$\mu(\mathbf{p}) := \frac{d(\mathbf{p}, \{f = 0\})}{|f(\mathbf{p})|} \in \left[1, \frac{1}{q}\right] \quad (\mathbf{p} \in \{f \neq 0\}),$$

where the range of  $\mu$  is obtained by writing the inequalities in (2) into the nominator above. Trivially,  $|f \cdot \mu|$  is a distance function because the right hand side of the

$$f(\mathbf{p}) \cdot \mu(\mathbf{p}) = f(\mathbf{p}) \cdot \frac{d(\mathbf{p}, \{f = 0\})}{|f(\mathbf{p})|} = \text{sgn}(f(\mathbf{p})) \cdot d(\mathbf{p}, \{f = 0\})$$

equation is continuous on the  $\{f \neq 0\}$  set.

3.⇒1. Because  $f \cdot \mu$  SDF is continuous, the function  $\text{sgn} \circ (f \cdot \mu) = (\text{sgn} \circ f) \cdot (\text{sgn} \circ \mu) = \text{sgn} \circ f$  is also continuous on the set  $\{f \neq 0\}$ .  $q \in \mathcal{F} f$  and  $1 \in \mathcal{C} f$  holds because  $\forall \mathbf{p} \in \mathbb{R}^3$ :

$$|f(\mathbf{p})| \cdot 1 \leq |f(\mathbf{p}) \cdot \mu(\mathbf{p})| = d(\mathbf{p}, \{f \cdot \mu = 0\}) = d(\mathbf{p}, \{f = 0\}) \leq |f(\mathbf{p})| \cdot \frac{1}{q}. \quad \square$$

## B PROOF WITHIN THE INTERIOR

*Proof of Theorem 2.* The fact that  $h$  is a signed distance lower bound was already proven by [17]. To prove out claim on the precision, first we show that if  $f(\mathbf{p}) \leq 0$  and  $g(\mathbf{p}) \leq 0$ , then

$$d(\mathbf{p}, h) = \min(d(\mathbf{p}, f), d(\mathbf{p}, g)). \quad (7)$$

Due to the Bolzano-property,  $\mathbf{p} \in f_0^- \Rightarrow d(\mathbf{p}, f) = d(\mathbf{p}, f_0^+)$ . So

$$\min(d(\mathbf{p}, f), d(\mathbf{p}, g)) = \min(d(\mathbf{p}, f_0^+), d(\mathbf{p}, g_0^+)) = d(\mathbf{p}, f_0^+ \cup g_0^+)$$

because of the definition of distance to a set. Using the de Morgan identity, one can reformulate the above for the intersection as

$$d(\mathbf{p}, f_0^+ \cup g_0^+) = d(\mathbf{p}, \mathbb{R}^3 \setminus (f^- \cap g^-)) = d(\mathbf{p}, \mathbb{R}^3 \setminus h^-) = d(\mathbf{p}, h_0^+) = d(\mathbf{p}, h).$$

using the Bolzano property again in the last equation. This proves that Equation (7) holds.

Second, let us prove that  $\min(q_f, q_g) \in \mathcal{F} h$  on the  $h_0^-$  set for  $q_f \in \mathcal{F} f$ ,  $q_g \in \mathcal{F} g$ . Because  $\mathbf{p} \in h_0^-$ , i. e.  $f(\mathbf{p}) < 0$  and  $g(\mathbf{p}) < 0$ , we have

$$|h(\mathbf{p})| = |\max(f(\mathbf{p}), g(\mathbf{p}))| = \min(|f(\mathbf{p})|, |g(\mathbf{p})|). \quad (8)$$

Finally, multiplying (7) with  $\min(q_f, q_g)$  and applying (8) leads to

$$\begin{aligned} \min(q_f, q_g) \cdot d(\mathbf{p}, h) &= \min(q_f, q_g) \cdot \min(d(\mathbf{p}, f), d(\mathbf{p}, g)) \\ &\leq \min(q_f, q_g) \cdot \min\left(\frac{1}{q_f}|f(\mathbf{p})|, \frac{1}{q_g}|g(\mathbf{p})|\right) \\ &\leq \min(q_f, q_g) \cdot \max\left(\frac{1}{q_f}, \frac{1}{q_g}\right) \cdot \min(|f(\mathbf{p})|, |g(\mathbf{p})|) \\ &= |h(\mathbf{p})|. \end{aligned}$$

Therefore,  $\min(q_f, q_g) \in \mathcal{F}(\max(f, g))$  on the  $f_0^- \cap g_0^-$  set. □

## C PROOF FOR FAR AWAY FROM THE SURFACE

*Proof of Theorem 3.* First, we derive an upper estimate of  $d(\mathbf{p}, h_0^-)$  with the exact distance to the bounded set  $d(\mathbf{p}, f_0^-)$ . Since  $h_0^- \subseteq f_0^-$ ,

$$d(\mathbf{p}, h_0^-) \leq d(\mathbf{p}, f_0^-) + \text{diam } f_0^- \quad (\mathbf{p} \in \mathbb{R}^3). \quad (9)$$

For the rest of the proof, let  $\mathbf{p} \in \mathbb{R}^3 \setminus \mathcal{K}_R(h_0^-)$ . Because  $R \leq d(\mathbf{p}, h_0^-)$ , and the assumption  $R > \text{diam } f_0^-$ , Equation (9) implies

$$0 < R - \text{diam } f_0^- \leq d(\mathbf{p}, f_0^-). \quad (10)$$

Second, we express a lower estimate of  $\max(f(\mathbf{p}), g(\mathbf{p}))$  using the distance  $d(\mathbf{p}, f_0^-)$ . Since  $f$  is an SDFE, let  $q_f \in \mathcal{F} f$ , so estimating  $\max(h(\mathbf{p}))$  yields

$$q_f \cdot d(\mathbf{p}, f_0^-) \leq f(\mathbf{p}) \leq \max(f(\mathbf{p}), g(\mathbf{p})). \quad (11)$$

Finally, we estimate the precision of the SDFE from the ratio of (9) and (11):

$$\begin{aligned}
 \frac{\max(f(\mathbf{p}), g(\mathbf{p}))}{d(\mathbf{p}, h_0^-)} &\geq \frac{q_f \cdot d(\mathbf{p}, f_0^-)}{d(\mathbf{p}, f_0^-) + \text{diam } f_0^-} \\
 &= q_f \cdot \frac{d(f_0^-, \mathbf{p}) + \text{diam } f_0^- - \text{diam } f_0^-}{d(\mathbf{p}, f_0^-) + \text{diam } f_0^-} \\
 &= q_f \left( 1 - \frac{\text{diam } f_0^-}{d(\mathbf{p}, f_0^-) + \text{diam } f_0^-} \right) \\
 &\geq q_f \cdot \frac{R - \text{diam } f_0^-}{R} \in \mathcal{F}h.
 \end{aligned}$$

For the last estimation Equation (10) was used. □

## D OFFSET DIFFERENCE SET

*Proof of Lemma 2.* Using the distance definition and that  $F = (F \setminus_{\frac{\delta}{2}} G) \cup (F \cap \overline{\mathcal{K}}_{\frac{\delta}{2}}(F \cap G))$ ,

$$d(\mathbf{p}, F) = \min \left( d(\mathbf{p}, F \setminus_{\frac{\delta}{2}} G), d(\mathbf{p}, F \cap \overline{\mathcal{K}}_{\frac{\delta}{2}}(F \cap G)) \right) \quad (12)$$

holds. However,  $F \cap \overline{\mathcal{K}}_{\frac{\delta}{2}}(F \cap G) \subseteq \overline{\mathcal{K}}_{\frac{\delta}{2}}(F \cap G)$ , so

$$d(\mathbf{p}, \overline{\mathcal{K}}_{\frac{\delta}{2}}(F \cap G)) \leq d(\mathbf{p}, F \cap \overline{\mathcal{K}}_{\frac{\delta}{2}}(F \cap G)). \quad (13)$$

Using the additivity of offsets and Theorem 1 for the set  $\overline{\mathcal{K}}_{\frac{\delta}{2}}(F \cap G)$  with  $r = \frac{\delta}{2}$ , so

$$d(\mathbf{p}, \overline{\mathcal{K}}_{\frac{\delta}{2}}(F \cap G)) - \frac{\delta}{2} = d(\mathbf{p}, \overline{\mathcal{K}}_{\delta}(F \cap G))$$

holds because  $\mathbf{p} \notin \mathcal{K}_{\delta}(F \cap G)$ . Therefore

$$\frac{\delta}{2} \leq d(\mathbf{p}, \overline{\mathcal{K}}_{\frac{\delta}{2}}(F \cap G)) \leq d(\mathbf{p}, F \cap \overline{\mathcal{K}}_{\frac{\delta}{2}}(F \cap G)) \quad (14)$$

Substituting (14) into (12) yields statement (3). □

## E SET CONTACT SMOOTHNESS LEMMA

*Proof of Lemma 3.* Using Lemma 2 on both  $F \setminus_{\frac{\delta}{2}} G$  and  $G \setminus_{\frac{\delta}{2}} F$ , and taking the maximum of the inequalities results in

$$\min \left( \frac{\delta}{2}, \max \left( d(\mathbf{p}, F \setminus_{\frac{\delta}{2}} G), d(\mathbf{p}, G \setminus_{\frac{\delta}{2}} F) \right) \right) \leq \max(d(\mathbf{p}, F), d(\mathbf{p}, G)) \quad (15)$$

Assume that  $F \setminus_{\frac{\delta}{2}} G$  and  $G \setminus_{\frac{\delta}{2}} F$  sets are not empty. Because these sets are closed, there exists  $\mathbf{x} \in F \setminus_{\frac{\delta}{2}} G$  and  $\mathbf{y} \in G \setminus_{\frac{\delta}{2}} F$  such that

$$d(\mathbf{p}, F \setminus_{\frac{\delta}{2}} G) = d(\mathbf{p}, \mathbf{x}) \quad \text{and} \quad d(\mathbf{p}, G \setminus_{\frac{\delta}{2}} F) = d(\mathbf{p}, \mathbf{y})$$

from Lemma 1. From the distance definition and the triangle inequality in  $\mathbf{xpy}$ , we estimate the maximum distance

$$\begin{aligned} 2 \max\left(d(\mathbf{p}, F \setminus_{\frac{\delta}{2}} G), d(\mathbf{p}, G \setminus_{\frac{\delta}{2}} F)\right) &= 2 \max(d(\mathbf{p}, \mathbf{x}), d(\mathbf{p}, \mathbf{y})) \geq \\ &\geq d(\mathbf{p}, \mathbf{x}) + d(\mathbf{p}, \mathbf{y}) \geq d(\mathbf{x}, \mathbf{y}) \geq d(F \setminus_{\frac{\delta}{2}} G, G \setminus_{\frac{\delta}{2}} F) = \sigma_{F,G}^*(\delta) \end{aligned}$$

Combining (15) and the inequality yields the estimate in the theorem.

If one of the  $F \setminus_{\frac{\delta}{2}} G$  and  $G \setminus_{\frac{\delta}{2}} F$  sets are empty, we get a lower estimate of  $\frac{\delta}{2}$  from (15). So the Lemma holds in this case because of property 3 in Proposition 2.  $\square$

## F PROOF ON THE DIFFERENCE SET

*Proof of Theorem 4.* Since we know that  $h$  is a distance bound of  $h_0^-$  from [17], we only have to prove that

$$\inf \left\{ \frac{h(\mathbf{p})}{d(\mathbf{p}, h_0^-)} : \mathbf{p} \in g_0^- \setminus_{\delta} f_0^- \right\} > 0$$

Let  $\mathbf{p} \in g_0^- \setminus_{\delta} f_0^-$ , so  $g(\mathbf{p}) \leq 0 \leq f(\mathbf{p})$ ; therefore,  $h(\mathbf{p}) = \max(f(\mathbf{p}), g(\mathbf{p})) = f(\mathbf{p})$ , and

$$\frac{h(\mathbf{p})}{d(\mathbf{p}, h_0^-)} = \frac{f(\mathbf{p})}{d(\mathbf{p}, h_0^-)} \geq q_f \cdot \frac{d(\mathbf{p}, f_0^-)}{d(\mathbf{p}, h_0^-)}$$

From Lemma 2 with  $F := f_0^-$ ,  $G := g_0^-$ , we can approximate the above further by

$$q_f \cdot \frac{d(\mathbf{p}, f_0^-)}{d(\mathbf{p}, h_0^-)} \geq q_f \cdot \frac{\min\left(\frac{\delta}{2}, d(\mathbf{p}, f_0^- \setminus_{\frac{\delta}{2}} g_0^-)\right)}{d(\mathbf{p}, h_0^-)} \quad (16)$$

Since  $\mathbf{p} \in g_0^- \setminus_{\delta} f_0^- \subseteq g_0^- \setminus_{\frac{\delta}{2}} f_0^-$ , then

$$d(\mathbf{p}, f_0^- \setminus_{\frac{\delta}{2}} g_0^-) \geq d(g_0^- \setminus_{\delta} f_0^-, f_0^- \setminus_{\frac{\delta}{2}} g_0^-) \geq d(g_0^- \setminus_{\frac{\delta}{2}} f_0^-, f_0^- \setminus_{\frac{\delta}{2}} g_0^-) = \sigma_{f_0^-, g_0^-}^*(\delta),$$

which implies the following using (16) and Definition 13:

$$q_f \cdot \frac{\min\left(\frac{\delta}{2}, d(\mathbf{p}, f_0^- \setminus_{\frac{\delta}{2}} g_0^-)\right)}{d(\mathbf{p}, h_0^-)} \geq q_f \cdot \frac{\sigma_{f_0^-, g_0^-}(\delta)}{d(\mathbf{p}, h_0^-)}.$$

Since  $d(\mathbf{p}, h_0^-) \leq R$ , the bound in (4) holds. The lower distance bound is positive because of property 4 in Proposition 2.  $\square$

## G PROOF IN THE EXTERIOR

*Proof of Theorem 5.* Let us estimate  $h(\mathbf{p})$  from below. Using the SDFE precision gives

$$\begin{aligned} \max(f(\mathbf{p}), g(\mathbf{p})) &\geq \max(q_f \cdot d(\mathbf{p}, f_0^-), q_g \cdot d(\mathbf{p}, g_0^-)) \\ &\geq \min(q_f, q_g) \cdot \max(d(\mathbf{p}, f_0^-), d(\mathbf{p}, g_0^-)) \\ &\geq \min(q_f, q_g) \cdot \frac{1}{2} \sigma_{f_0^-, g_0^-}(\delta) \\ &\geq \min(q_f, q_g) \cdot \frac{1}{2} \sigma_{f_0^-, g_0^-}(\delta) \cdot \frac{d(\mathbf{p}, h_0^-)}{R} \end{aligned}$$

Lemma 3 and the  $d(\mathbf{p}, h_0^-) < R$  condition gave the precision which is positive because of property 4 in Proposition 2.  $\square$

## H PROOF FOR SUMMARY OF SET OPERATIONS

*Proof of Theorem 6.* If  $f_0^\pm$  is bounded and  $f_0^\mp$  is not, then  $\text{diam } f_0^\pm = \text{diam}\{f = 0\}$ . Equation (6) holds if we replace  $f$  by  $-f$  and  $g$  by  $-g$ , so it is enough to prove the proposition for  $h = \max(f, g)$ , since that implies the case of the union and the set difference. Theorem 2 implies that

$$\min(q_f, q_g) \in \mathcal{F}h \Big|_{h_0^-}. \quad (17)$$

Since  $f_0^- \setminus g_0^- \subseteq f_0^- \subseteq \bar{\mathcal{K}}_{\text{diam } f_0^-}(h_0^-)$ , Theorem 4 with  $R = \text{diam } f_0^-$  implies

$$\frac{\sigma_{f_0^-, g_0^-}(\delta)}{\text{diam } f_0^-} \cdot q_g \in \mathcal{F}h \Big|_{f_0^- \setminus \delta g_0^-}. \quad (18)$$

In Theorems 3, 4, and 5, let  $R := 2 \text{diam } f_0^-$ , so that

$$\begin{aligned} \frac{1}{2} q_f &\in \mathcal{F}h \Big|_{\mathbb{R}^3 \setminus \mathcal{K}_{2 \text{diam } f_0^-}(h_0^-)}, \\ \frac{1}{2} \frac{\sigma_{f_0^-, g_0^-}(\delta)}{\text{diam } f_0^-} \cdot q_f &\in \mathcal{F}h \Big|_{(g_0^- \setminus \delta f_0^-) \cap \mathcal{K}_{2 \text{diam } f_0^-}(h_0^-)}, \\ \frac{1}{4} \frac{\sigma_{f_0^-, g_0^-}(\delta)}{\text{diam } f_0^-} \cdot \min(q_f, q_g) &\in \mathcal{F}h \Big|_{(f_0^+ \cap g_0^+) \setminus \delta h_0^- \cap \mathcal{K}_{2 \text{diam } f_0^-}(h_0^-)}. \end{aligned}$$

For the union of sets on the right hand side of Equations (17), (18), and (H), we need to take the minimum value of the precision values on the left. Since  $\sigma_{f_0^-, g_0^-}(\delta) \leq \delta \leq \text{diam } f_0^-$ , the last value is always the smallest of the four. Therefore,

$$\frac{1}{4} \frac{\sigma_{f_0^-, g_0^-}(\delta)}{\text{diam } f_0^-} \cdot \min(q_f, q_g) \in \mathcal{F}h \Big|_{\mathbb{R}^3 \setminus \mathcal{K}_\delta(h_0^-) \cup h_0^-}.$$

Finally, note that  $\mathbb{R}^3 \setminus \mathcal{K}_\delta(\{h = 0\}) \subseteq \mathbb{R}^3 \setminus \mathcal{K}_\delta(h_0^-) \cup h_0^-$ , and that  $\sigma_{\{f=0\}, \{g=0\}}(\delta) \leq \sigma_{f_0^-, g_0^-}(\delta)$  because  $\{f = 0\} \subseteq f_0^-$  and  $\{g = 0\} \subseteq g_0^-$ .  $\square$